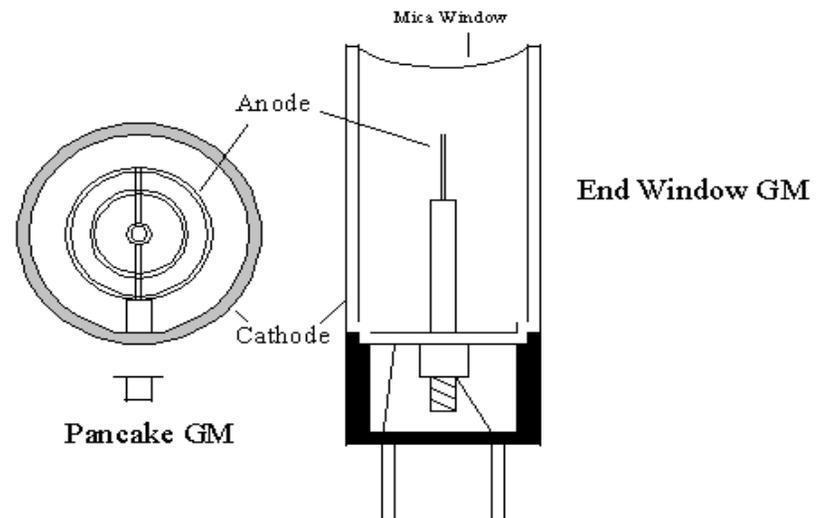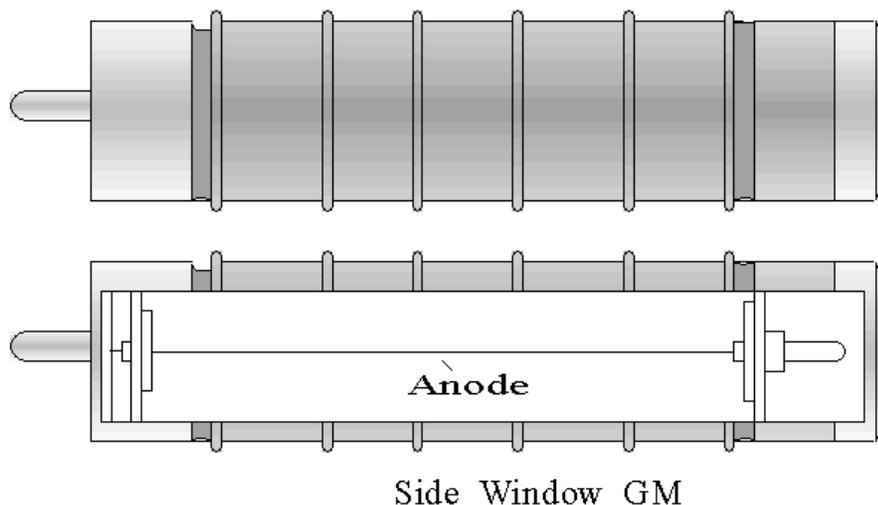# Geiger Mueller

The essential components of the Geiger-Mueller detector are its two collecting electrodes: the anode and cathode. In most cases, the outer chamber is
It can be used to count gamma, beta and alpha exposure rates.

Side window: Stainless steel cathode + tungsten wire. If the side window (30 mg/cm^2) is thin enough not only gamma but also beta

Pancake: truncated cylinder. One end covered with thin mica window. Circular anode in a plane parallel to entrance window. End Window: stainless steel cylinder with anode at 1 end. Window size: 1.5-2 mg/cm^2 also for beta and alpha

Anode

Side Window GM

Mica Window

Anode

Cathode

Pancake GM

End Window GM

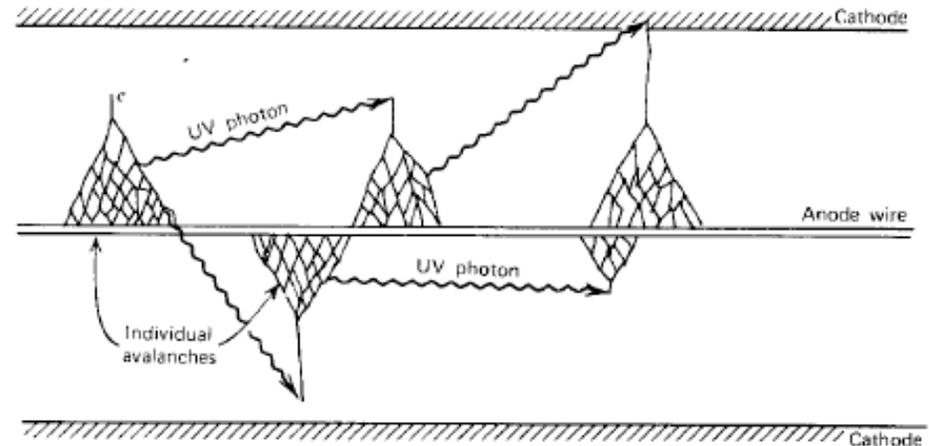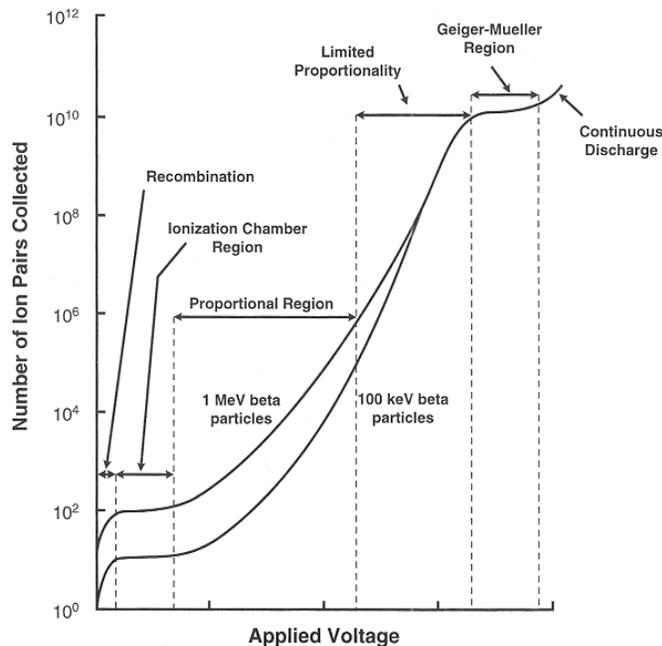# Geiger Mueller

Pressure of gas around few tens of atmospheres

Gas filling: 2 components primary (Ne, Ar, Kr, He, …) and quencher (halogen gases, isobutane,…)

When a ionizing particle (beta or alpha) gets through the detector window it ionizes the gas. Gamma or X-rays ionize the gas indirectly interacting in the metal walls (photoelectric effect, pair production or Compton) so that an electron is knocked off the walls. The electric field accelerate electrons and they acquire enough kinetic energy to ionize further the gas. The electrons produced in these secondary ion pairs, along with the primary electrons, continue to gain energy as they move towards the anode and produce more and more ionizations. The result is that each electron from a primary ion pair produces a cascade or avalanche of ion pairs (Townsend avalanche).

If the electric field strength is higher than what used in the proportional mode, the number of UV photons formed in the avalanche process increases considerably. They are formed since not only there is secondary ionization, but also excitation of atmos that emit UV photon in their de-excitation.These create photoelectrons in the whole gas and in the walls of the counter. The avalanche spreads over the whole counter and leads to a complete discharge. Secondary avalanches are induced and they envelope the anode.

Geiger Mueller

The number of electrons produced is independent of the applied voltage and independent on the primary ionization. When the Geiger-Mueller region sets in (gas amplification of about 10^8-10^{10}) the number of ion pairs liberated then becomes equal for particles inducing different primary ionization, namely electrons or α. These counters do not allow to discriminate incoming particles.
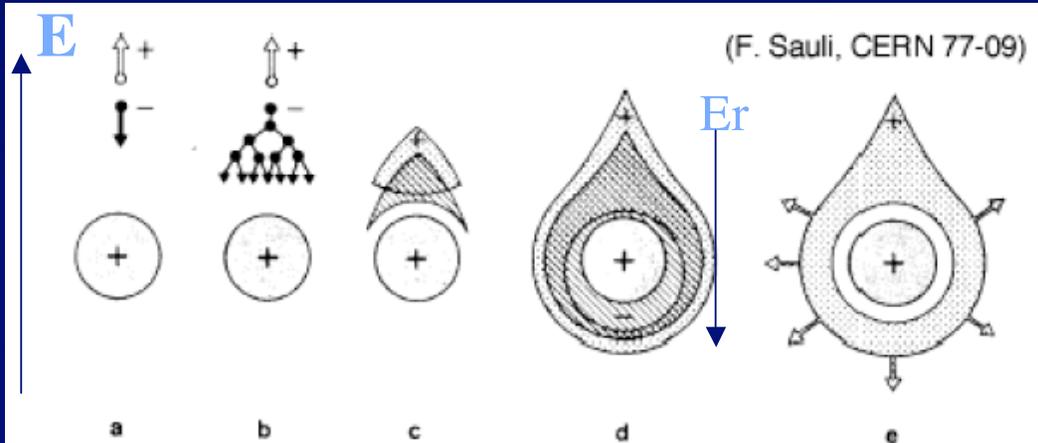
Streamer tubes

They operate in the intermediate region between the proportional one and the Geiger-Mueller. They are gas filled chambers with 2 planar electrodes. A very strong electric field E>40 kV/cm is applied to the plates

The charged particle traverses the detector and a cluster of ionization electrons is formed. This develops in an avalanche that grows at a speed of 10^7 cm/s. A drop shaped avalanche forms owing to the different mobility of electrons and ions. The electric field E_r due to the space charge in the avalanche adds to the external field E. In the combined field $E+E_r$, UV photons emitted by excited atoms can produce secondary avalanches. Secondary and primary ones merge to form 2 plasma channels, 1 growing towards the anode and the other towards the anode. The streamers can reach the electrodes and cause a spark.

External quenching can be used decreasing the voltage or mixtures of gases containing quenchers

(F. Sauli, CERN 77-09)

Summary on spatial and time resolutions

Table 27.1: Typical spatial and temporal resolutions of common detectors.

Detector Type	Accuracy (rms)	Resolution Time	Dead Time
Bubble chamber	10 to 150 μm	1 ms	50 ms[a]
Streamer chamber	300 μm	2 μs	100 ms
Proportional chamber	$\geq 300~\mu$m[b,c]	50 ns	200 ns
Drift chamber	50 to 300 μm	2 ns[d]	100 ns
Scintillator	—	150 ps	10 ns
Emulsion	1 μm	—	—
Silicon strip	$\dfrac{\text{pitch}}{\text{3 to 7}}$[e]	[f]	[f]
Silicon pixel	2 μm[g]	[f]	[f]

[a] Multiple pulsing time.

[b] 300 μm is for 1 mm pitch.

[c] Delay line cathode readout can give $\pm 150~\mu$m parallel to anode wire.

[d] For two chambers.

[e] The highest resolution ("7") is obtained for small-pitch detectors ($\lesssim 25~\mu$m) with pulse-height-weighted center finding.

[f] Limited at present by properties of the readout electronics. (Time resolution of ≤ 25 ns is planned for the ATLAS SCT.)

[g] Analog readout of 34 μm pitch, monolithic pixel detectors.

Measurement of Momentum in a magnetic field

$$\underline{F} = Q\underline{v} \times \underline{B}$$

$$\underline{F} = \frac{d\underline{p}}{dt}$$

$$\underline{p} = \gamma m\underline{v} \implies \frac{d\underline{p}}{dt} = \gamma m \frac{d\underline{v}}{dt}$$

If the velocity is orthogonal to the field:

$$\frac{dv}{dt} = \frac{v^2}{r} = \frac{F}{vm} = \frac{QvB}{vm}$$

The trajectory is a circumference with radius

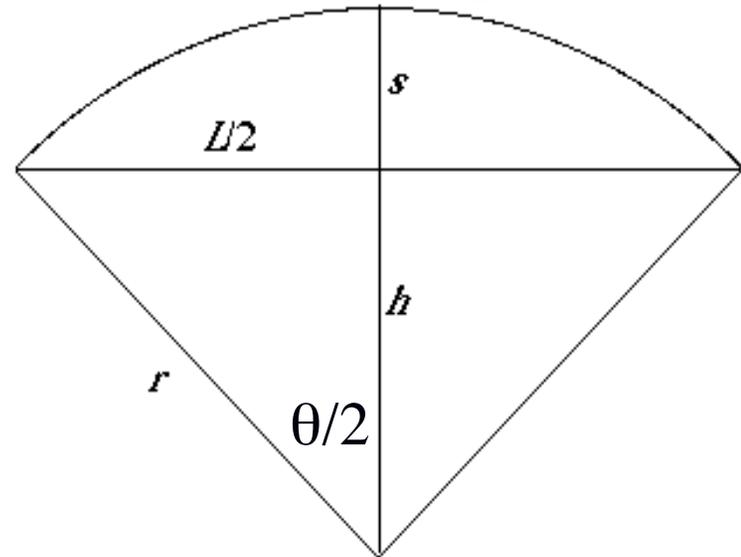$$r = \frac{\gamma m v^2}{QvB} = \frac{\gamma m v}{QB} = \frac{p}{QB}$$

If the velocity forms an angle θ with the direction of the field, the trajectory is a helix with radius

$$r = \frac{p\sin\theta}{QB}$$

Lets consider a particle of momentum p passing through a region of length L with a magnetic field B . The deviation from a straight line is the sagitta s of the track.

$$s = R - R\cos\frac{\theta}{2} \approx \frac{R\theta^2}{8}$$

$$1 - \cos\frac{\theta}{2} = 2\sin^2\frac{\theta}{4} \approx \frac{\theta^2}{8}$$

Momentum Measurement

$$s = R - R\cos\frac{\theta}{2} \approx \frac{R\theta^2}{8}$$

$$s \approx \frac{R(QBL)^2}{8p^2} = \frac{QBL^2}{8p}$$

$$1 - \cos\frac{\theta}{2} = 2\sin^2\frac{\theta}{4} \approx \frac{\theta^2}{8}$$

The momentum error is connected to the error on the measurement of the sagitta

$$\left|\frac{dp}{ds}\right| = \frac{L^2 QB}{8s^2} = \frac{p}{s}$$

$$\Rightarrow \delta p = \frac{p}{s}\delta s$$

$$\text{or} \quad \frac{\delta p}{p} = \frac{\delta s}{s}$$

$$\frac{\sigma(P)}{P} = \frac{\sigma(s)}{s} \approx \frac{\sqrt{3}\sigma(x)8P}{eBL^2}$$

The fractional error on the momentum is proportional to the momentum of the particle (multiple scattering is neglected)

Calorimeters

Fabian and Giannotti

http://doc.cern.ch/archive/electronic/cern/preprints/ep/ep-2003-075.pdf
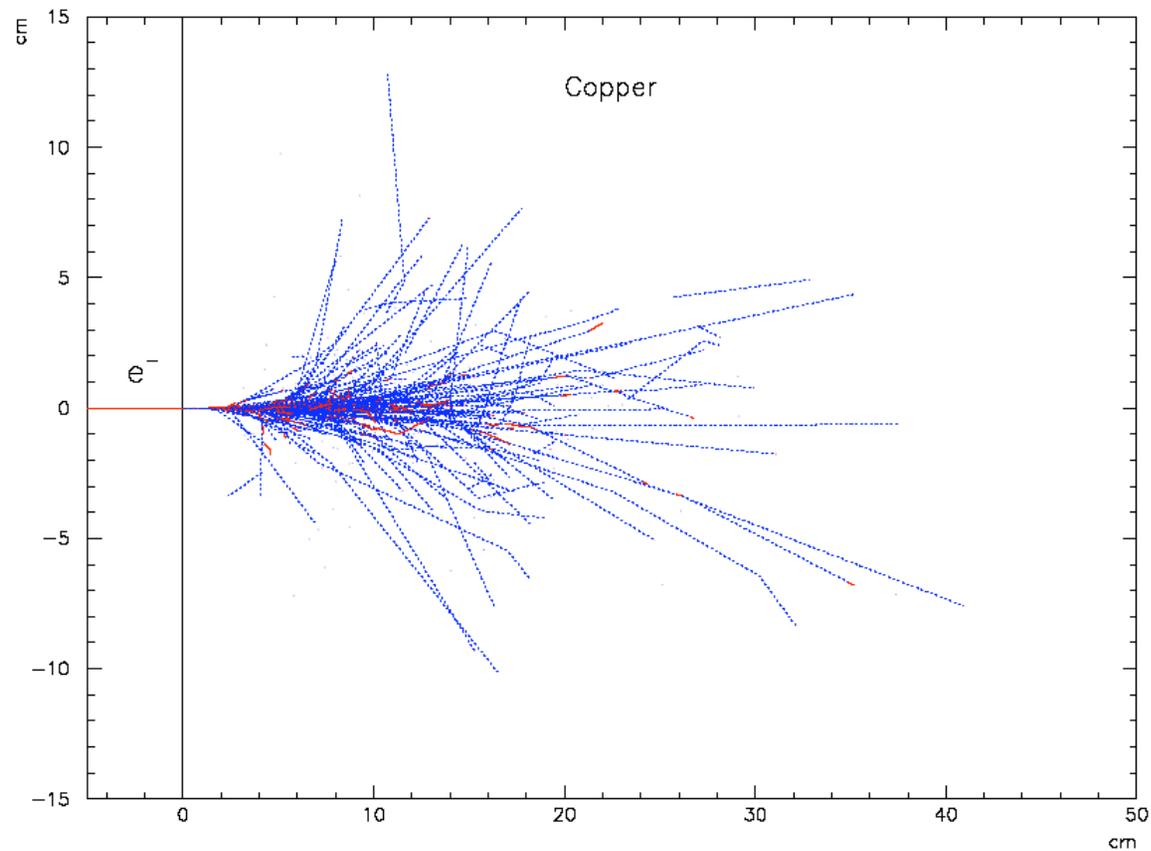
Originally invented for Cosmic Rays studies, now applied much in accelerator physics to measure the energy of photons, electrons and hadrons

Calorimeters are instrumented blocks of matter in which the particle interacts and deposits all its energy in the form of a cascade of particles whose energy decreases progressively down to the energy at which ionization and excitations dominate. The deposited energy is detectable in the form of a signal proportional to the incoming energy. They can even measure the position and angle of the incident particle.

The different response to electrons, muons and hadrons can be used for pid. Neutrinos are measured through missing energy.
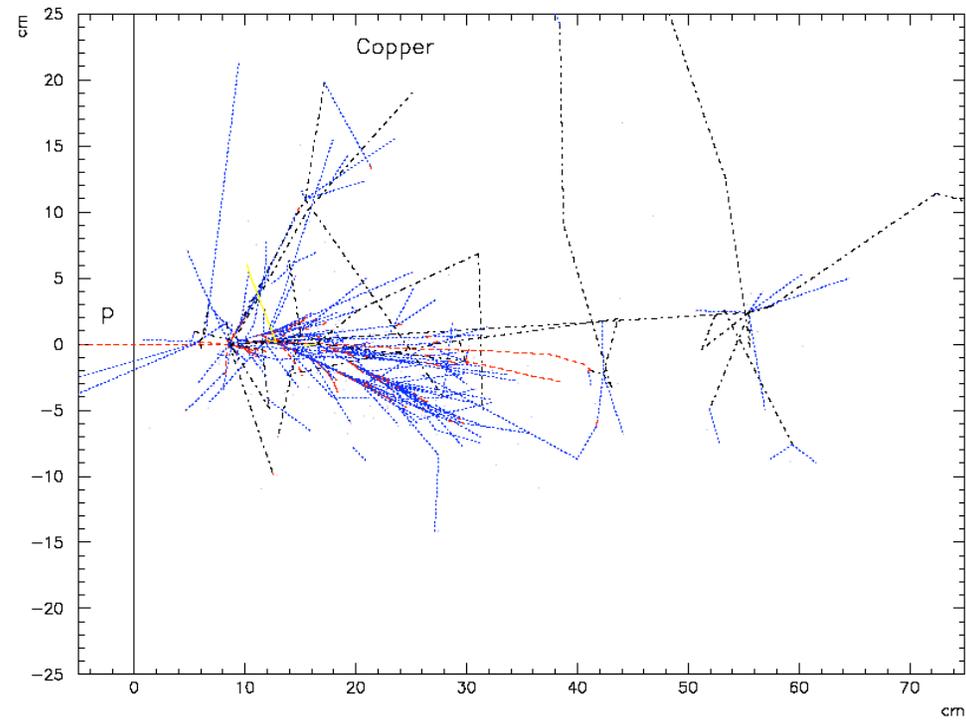
Electron in Medium

Trajectory of 8 GeV e$^-$ in copper.
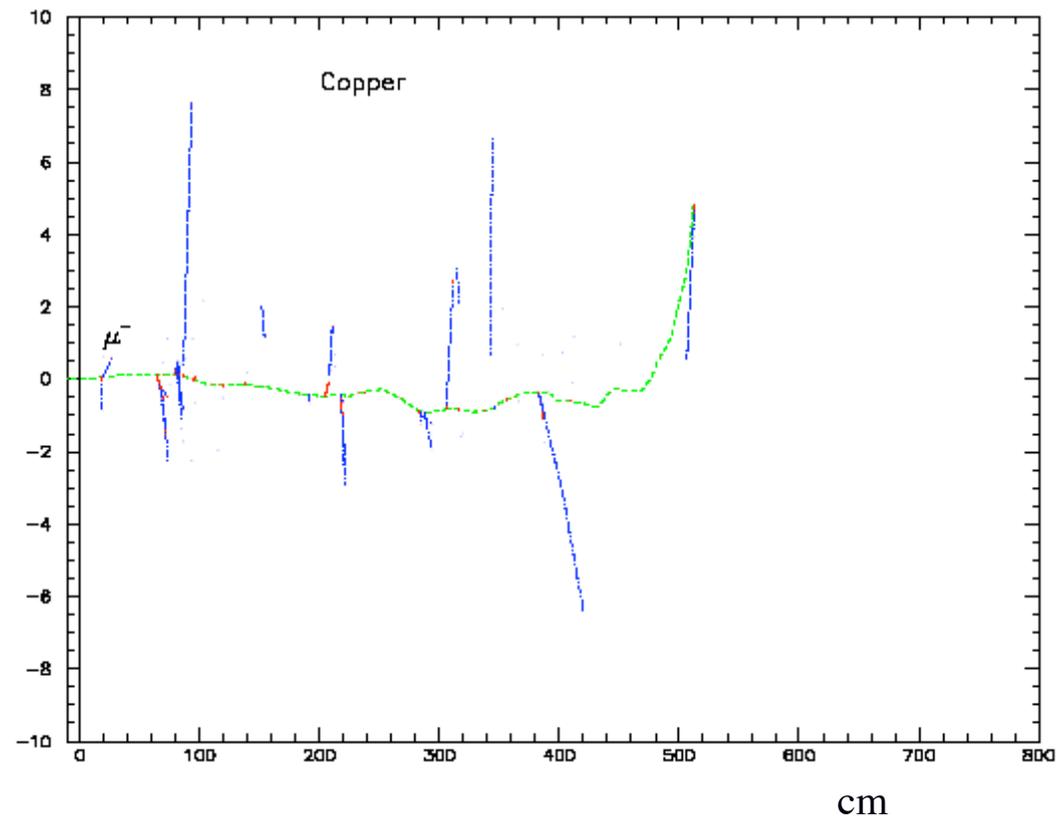The coordinates are in cm.

Proton in Medium

Trajectory of 8 GeV proton in copper.

The coordinates are in cm.

Muon in medium

Trajectory of 8 GeV μ^- in copper.

The coordinates are in cm.

cm

Calorimeter classification

Electromagnetic calorimeters measure the energy released by em interacting particles (electrons, positrons, photons) through their em interactions (eg. bremsstrahlung and pair production)

Hadronic calorimeters measure the energy of hadrons (eg. pions, protons) through their strong and em interactions.

Homogeneous calorimeters: unique block of sensitive material (lead-glass, NaI sodium-iodide crystal, bismuth-germanium oxide BGO crystal)

Sampling calorimeters when the energy is measured by sensitive layers interspersed with absorbing material layers that speed up the cascade process Active medium can be scintillators, Si, LAr, gas,…and absorbers (Fe, Cu, Pb, U,…)

The longitudinal depth of calorimeters varies as lnE so they can remain compact objects and the lateral dimensions should be large enough to avoid leakage of cascades.

Electromagnetic showers

In contrast to magnetic spectrometers, where $\sigma(p)/p \propto p$ the resolution deteriorates linearly with p, the calorimeter energy resolution improves with energy as $1/\text{sqrt}(E_0)$, E_0 = energy of incident particle

We know the em shower is governed by

$$X_0(g/cm^2) = \frac{716A}{Z(Z+1.3)\left(\ln\frac{183}{Z^{1/3}} + \frac{1}{8}\right)} = \frac{A}{N_A \sigma_{bremss}}$$

That is the distance necessary to reduce by 1/e the energy of the particle

$$\langle E(x) \rangle = E_0 \, e^{-\frac{x}{X_0}}$$

The mean longitudinal profile is

$$\frac{dE}{dt} = E_0 b \frac{(bt)^{a-1} e^{-bt}}{\Gamma(a)}$$

$$t = x/X_0$$

and a and b depend on the nature of the incident particle
The shower maximum is log dependent on the energy

$$t_{max} \simeq \ln \frac{E_0}{\epsilon} + t_0$$

with t_0 = -0.5 (0.5) for electrons (photons)
A measurement of the transverse size is the Moliere radius: a cylinder of radius that contains on average 90% of the shower energy

$$R_M \ (g/cm^2) \simeq 21 \ \text{MeV} \frac{X_0}{\epsilon(\text{MeV})}$$

Energy resolution of an em calorimeter

The total track length T_0 is proportionl to the energy E_0

$$T_0 \ (\mathrm{g/cm^2}) \div X_0 \frac{E_0}{\epsilon}$$

Where E_0/ϵ = number of particles in the shower

E_0 can be measured using the scintillation light produced by charged tracks or the charge produced in a gas detector The resolution is mainly limited by fluctuations in T_0 (that is proportional to the number of tracks in the shower)

$$\sigma(E) \div \sqrt{T_0}$$

Hence

$$\frac{\sigma(E)}{E} \div \frac{1}{\sqrt{T_0}} \div \frac{1}{\sqrt{E_0}}$$

Quadratic sum

In the reality other factors deteriorate the energy resolution

$$\frac{\sigma}{E} = \frac{a}{\sqrt{E}} \oplus \frac{b}{E} \oplus c$$

$\frac{a}{\sqrt{E}}$ = stochastic term above $\frac{b}{E}$ = noise term c = constant term

Energy resolution of an em calorimeter

$$\frac{\sigma}{E} = \frac{a}{\sqrt{E}} \oplus \frac{b}{E} \oplus c$$

$\frac{a}{\sqrt{E}}$ = stochastic term: typically it is few %/sqrt(E(GeV)) in homogeneus calorimeters

In sampling calorimeters there are fluctuations due to absorber layers that can be determined counting the charged particles crossing active layers that is proportional to the incident particle energy (t = thickness of absorber layers in units of X_0)

$$N_{ch} \div \frac{E_0}{t} ,$$

The smaller t the better the energy resolution

$$\frac{\sigma}{E} \div \frac{1}{\sqrt{N_{ch}}} \div \sqrt{\frac{t}{E_0(\text{GeV})}} \qquad \text{typically} \qquad 5\text{--}20\%/\sqrt{E(\text{GeV})}$$

The noise term $\frac{b}{E}$ comes from the electronic noise of the readout chain

The constant term depends on nonuniformities of the detector whose response may vary eg with the impact position, caused by ageing, T gradients, imperfections…should be kept at % level

An example

$$\sigma(E)/E = \sqrt{(a^2/E + (b/E)^2 + c^2)}$$
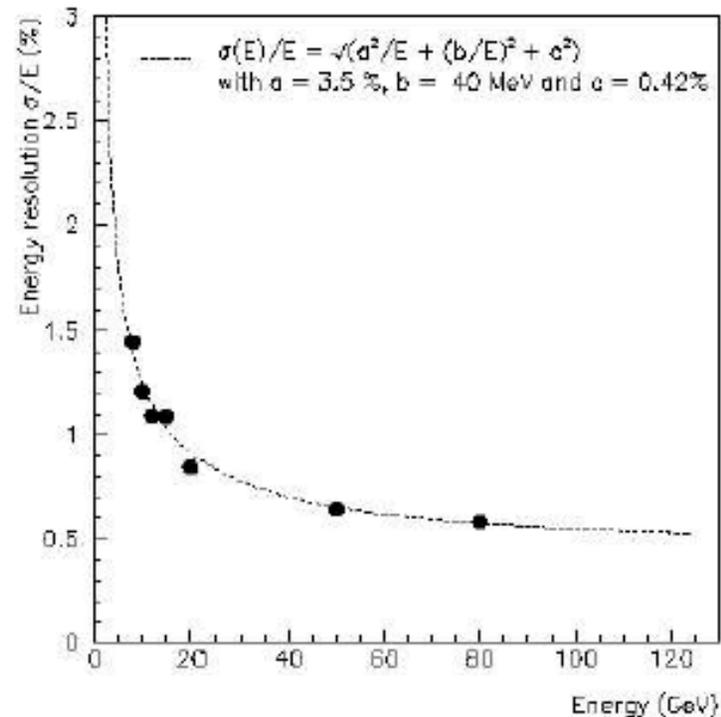with $a = 3.5\ \%$, $b = 40\ \text{MeV}$ and $c = 0.42\%$

FIG. 3 Fractional electron energy resolution as a function of energy measured with a prototype of the NA48 liquid krypton electromagnetic calorimeter (NA48 Collaboration, 1995). The full line is a fit to the experimental points with the form and the parameters indicated in the figure.

Additional contributions come from energy longitudinal and lateral leakages

Typical energy resolutions of em calorimeters

Table 27.5: Resolution of typical electromagnetic calorimeters. E is in GeV.

Detector	Resolution
NaI(Tl) (Crystal Ball [72]; 20 X_0)	$2.7\%/E^{1/4}$
Lead glass (OPAL [73])	$5\%/\sqrt{E}$
Lead-liquid argon (NA31 [74]; 80 cells: 27 X_0, 1.5 mm Pb + 0.6 mm Al + 0.8 mm G10 + 4 mm LA)	$7.5\%/\sqrt{E}$
Lead-scintillator sandwich (ARGUS [75], LAPP-LAL [76])	$9\%/\sqrt{E}$
Lead-scintillator spaghetti (CERN test module) [77]	$13\%/\sqrt{E}$
Proportional wire chamber (MAC; 32 cells: 13 X_0, 2.5 mm typemetal + 1.6 mm Al) [78]	$23\%/\sqrt{E}$

Non uniformities, leakages, statistics

Homogeneous calorimeters

•Semiconductor calorimeters: ionization tracks produce hole-electron couples, excellent energy resolutions. Examples are Si and Ge crystals

$N_{eh} = E_0/W$

$$\frac{\sigma}{E} \doteq \frac{\sqrt{F}}{\sqrt{N_{eh}}}$$

F = 0.13 for Ge

•Cherenkov calorimeters: transparent material in which relativistic $e^{\pm}$ produce Cherenkov photons, eg. lead glass PbO: easy to handle but not resistant to radiation exposure. 1000 pe/GeV $\Rightarrow$ $\sim 3\%/\sqrt{E(\text{GeV})}.$

In SK 60 pe/MeV and at 10 MeV resolution 20% for electrons

•Scintillator counters: ionization tracks produce light (fluorescence) Eg. BGO, CsI, $PbWO_4$ crystals. Organic lower light yield, inorganic higher light yield but slower. NaI(Tl) has been much used for low cost and high light yield, but has long X_0 and hygroscopic. For more compact detectors better BGO. Also CsI (Tl) is very popular $\simeq 2\%/E^{1/4} \oplus 1.8\%$ in BaBar

Homogeneous calorimeters

•Noble liquid calorimeters (Ar, Kr, Xe operated at cryogenic temperature). Large scale calorimeters are based on charge measurement, though also scintillation can be collected (about 50% of the energy loss)
If only ionization is read out

$$\sigma(N_{\mathrm{ion}}) = \sqrt{N \frac{N_{\mathrm{ion}}}{N} \frac{N_{\mathrm{scint}}}{N}} \qquad N = N_{\mathrm{ion}} + N_{\mathrm{scint}}$$

If 80% in ionization and 20% in scintillation

$$\sigma(N_{\mathrm{ion}}) \sim 0.4 \sqrt{N}.$$

2.5 better than for the pure behavior

$$1/\sqrt{N}$$

Properties of materials

Material	Density g/cm^3	X_0 g/cm^2	X_0 cm	λ_I g/cm^2	Molière $R_M\,cm$	E_{crit} MeV	Refr. index
W	19.3	6.5	0.35	185.	0.69	10.6	
Pb	11.3	6.4	0.56	194.	1.22	9.6	
Cu	8.96	13.	1.45	134.	1.15	26.	
Al	2.70	24.	8.9	106.	3.3	56.	
C	2.25	42.	18.8	86.	3.5	111.	
Plastic	1.0	44.	42.	82.	6.1		1.58
H_2	0.07	61.	860.	50.	50.	360.	

TABLE II Main properties of liquid argon, krypton and xenon.

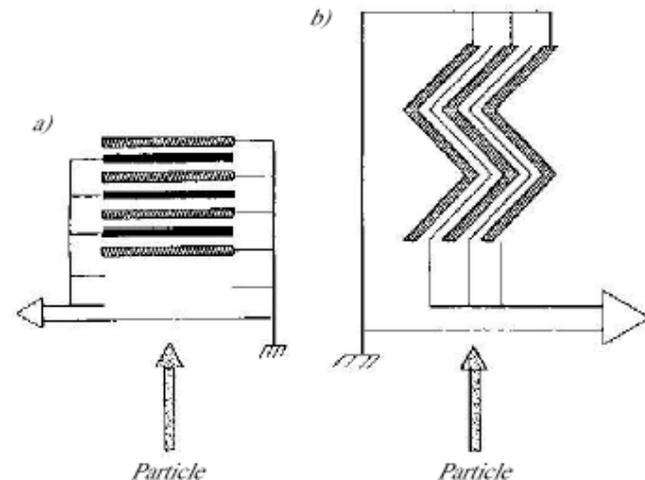|	Ar	Kr	Xe
Z	18	36	58
A	40	84	131
X_0 (cm)	14	4.7	2.8
R_M (cm)	7.2	4.7	4.2
Density (g/cm^3)	1.4	2.5	3.0
Ionization energy (eV/pair)	23.3	20.5	15.6
Critical energy ϵ (MeV)	41.7	21.5	14.5
Drift velocity at saturation (mm/μs)	10	5	3

Sampling calorimeters

Used always for hadronic showers since they allow reasonable dimensions <2m

•Scintillation sampling calorimeters: use plastic scintillators (cheap but suffer from radiation damage). Eg CLOE (DaΦhne): lead-scintillator calorimeter with 0.5 mm Pb layers in which 1 mm of fibers are embedded $\sigma/E \simeq 5\%/\sqrt{E(\text{GeV})}$

•Gas sampling calorimeters: operation in proportional mode is often important due to their low density media, difficult to achieve stability $(\lesssim 20\%/\sqrt{E(\text{GeV})})$

•Solid-state sampling calorimeters: high density also for active layer (>1000 than gas calorimeters), but high cost and poor radiation resistance

Sampling calorimeters

•Liquid sampling calorimeters: they are easy to calibrate since the active medium is very uniform. They are radiation resistant, but they need to be operated cryogenically, require high purity.They have slow collection time so only a part of the signal can be collected to be faster (50 ns) RC<<tc.
•So cables (that introduce high C) must be kept short but with the geometry a) long cables are needed to gang together successive layers. A geometry like in b) (accordion) can solve the problem since the signal can be extracted from the front and back faces of the calorimeter minimizing cables and connections.
Absorber and detectors are orthogonal to the particle
Electrodes must be bent in order not to have
particle leakage through Ar layers without
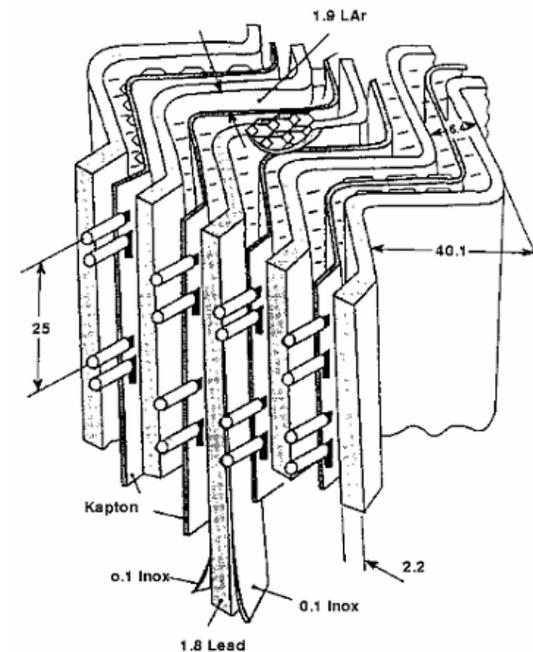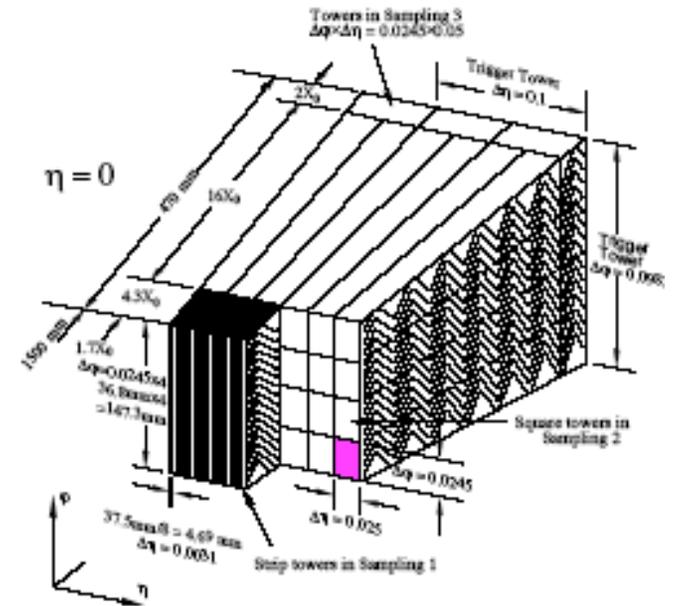crossing the absorber

ATLAS calorimeter

LAr em calorimeter (ATLAS):
inner barrel cylinder of 45 m³ and 2
end-caps of 19 m³ each, using the
intrinsically radiation resistant LAr
technology. The barrel part of the liquid
calorimetry is an e.m. `accordion'
calorimeter. with flat absorber plates,
and a forward calorimeter with a tube
electrode structure.
The calorimeter has an em shower
resolution 10%/sqrt(E(GeV))+0.25/E(GeV)+0.3%
CMS has put the goal on an excellent
energy resolution and chose semiconductor
detectors

- 2 mm Pb, 3 mm LAr
- 2-5 kV on the gaps

Hadronic Calorimeters

Mean free path between interactions

$$\lambda \approx 35\, A^{1/3}\, \mathrm{g\ cm^{-2}}$$

$$x/\lambda_I \equiv t_{\max} \approx 0.2 \ln(E/1\ \mathrm{GeV}) + 0.7$$

17.1 cm Fe, 18.5 cm in Pb, 34 cm in C, 12 cm in U

Photons, neutrons and neutrinos (also muons) that do not interact produce an invisible energy.

The energy deposit in a hadronic shower consists of a prompt em component due to π^0 production and a slower component due to the hadronic activity.

$$E_{\mathrm{vis}}^{\pi} = \eta_e F_{\pi^0} E + \eta_h F_h E$$

For a pion induced shower:

η = efficiency for observing a signal E_{vis}

F = fraction of particles

$$= \eta_e \left(F_{\pi^0} + \frac{\eta_h}{\eta_e} F_h \right) E ,$$

$$\eta_e \neq \eta_h \qquad E_{\mathrm{vis}}^{e} = \eta_e\, E$$

The e/π fraction of visible energy

$$\frac{E_{\mathrm{vis}}^{\pi}}{E_{\mathrm{vis}}^{e}} = \left(\frac{e}{\pi}\right)^{-1} = F_{\pi^0} + \frac{\eta_h}{\eta_e} F_h = (1 - F_h) + \frac{\eta_h}{\eta_e} F_h = 1 - \left(1 - \frac{\eta_h}{\eta_e}\right) F_h$$

F_h decreases with energy so the average response of an hadronic calorimeter will not be linear with energy. Event by event fluctuations in F_h and F_{π^0} (non gaussian) affect the energy resolution.

Compensation

On average the energy measurable for an hadronic shower is less than for an em one $e/\pi > 1$.

If $e/\pi \neq 1$. the energy resolution has the form $\sigma/E = a_1/\sqrt{E} \oplus a_2$.

Visible energy is incomplete because:

- muons, neutrinos escape
- Inelastic collisions result in low energy γ-rays, nuclear fragments, p and n that are absorbed in absorber layers without producing visible energy: non relativistic protons release energy 10-100 > mip, heavy nuclear fragments have short ranges and may stop in absorber layers leaving no visible energy. Neutrons release visible energy if the detector material contains H since on average 1/2 of the n kinetic energy is transferred to the recoil p in elastic scatterings n-p

It is possible to tune the response of calorimeters to achieve $e/\pi = 1$ (compensated) by choosing materials and thickness of active/passive layers. Two methods are generally used:
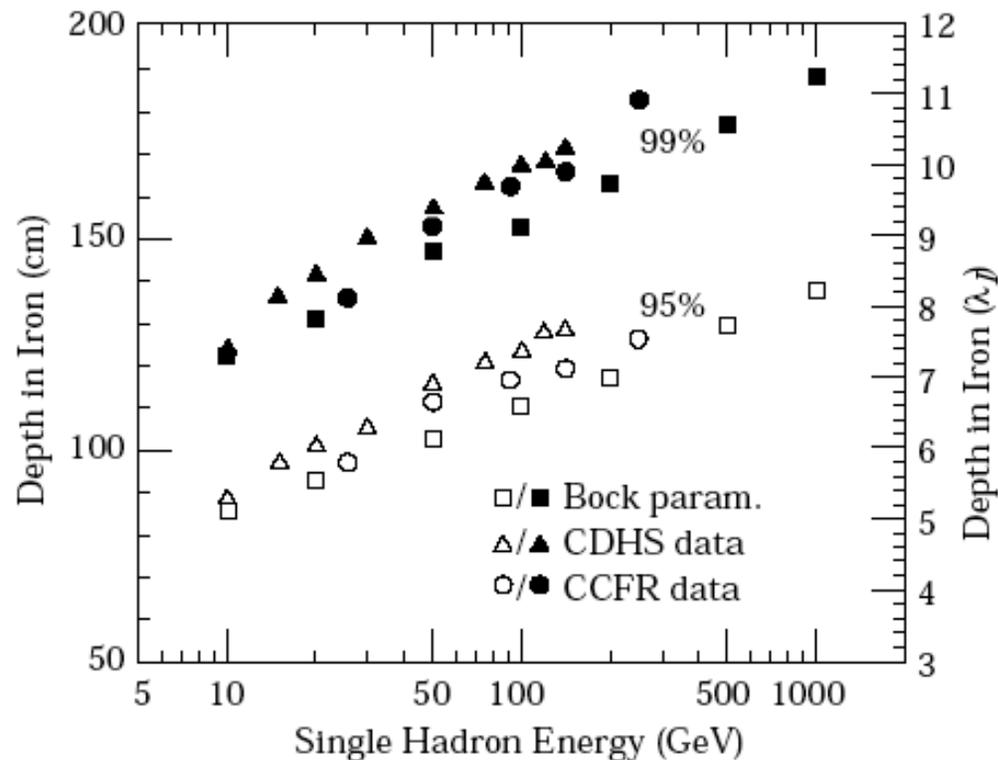
1) The loss of visible energy induced by nuclear reactions induced by shower particles may be compensated using ^{238}U. Its fission liberates n and γ so contributions from p recoils. Also the em signal decreases in high Z materials.
2) H rich materials 3) weighting responses of individual counters

On average the energy measurable for an hadronic shower is less than for an em one e/π >1.

It is possible to tune the response of calorimeters to achieve e/π = 1 (compensated) by chosing materials and thickness of active/passive layers

If $e/\pi \neq 1.$ the energy resolution has the form $\sigma/E = a_1/\sqrt{E} \oplus a_2$,

Dimensions of hadronic calorimeters

Energy resolution of Hadronic Calorimeters

For sampling calorimeters (ΔE = energy lost in one sampling)

$$\sigma_{\mathrm{samp}}/E = c \cdot (\Delta E(\mathrm{MeV})/E(\mathrm{GeV}))^{1/2}$$

For em ones: c = 0.05-0.06

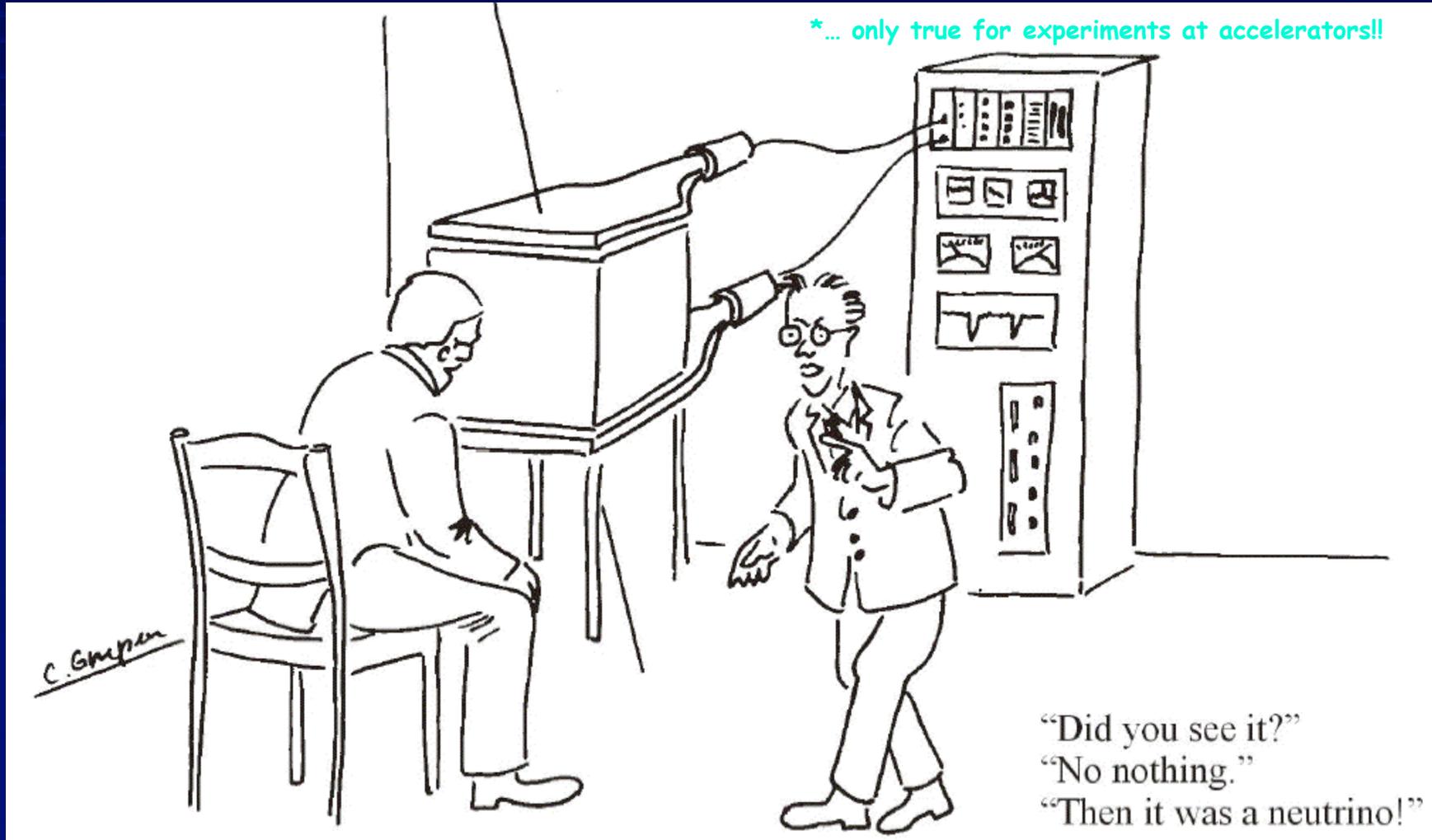For an hadronic cascade $c(\pi)$ ~0.09

For an hadronic calorimeter the resolution can be as good as $(\sigma/E) \cdot \sqrt{E} \lesssim 0.2$;

And sampling fluctuations contribute at the level of

$$\sigma/E \approx 0.09(\Delta E(\mathrm{MeV})/E(\mathrm{GeV}))^{1/2}.$$

A short word on neutrinos*…

*… only true for experiments at accelerators!!

"Did you see it?"
"No nothing."
"Then it was a neutrino!"

Suggested readings

Particle detectors

Konrad Kleinknecht, Detectors for Particle Radiation (2nd edition)

C. Leroy and PG Rancoita, Principles of Radiation Interaction in Matter and detection, World Scientific, 2004

G.F. Knoll, Radiation Detection and Measurement, ed. Wiley,Third edition, 2000

R.K. Bock & A. Vasilescu - The Particle Detector BriefBook, Springer 1998

Online:
http://pdg.lbl.gov/2005/reviews/pardetrpp.pdf
http://physics.web.cern.ch/Physics/ParticleDetector/BriefBook/
http://www.shef.ac.uk/physics/teaching/phy311/#books
http://www-physics.lbl.gov/%7Espieler/physics_198_notes_1999/index.html
http://besch2.physik.uni-siegen.de/%7Edepac/DePAC/DePAC_tutorial_database/grupen_istanbul/grupen_istanbul.html